Am J Transl Res 2012;4(1):24-43
www.ajtr.org /ISSN:1943-8141/AJTR1112003

Original Article

An atlas of histone deacetylase expression in breast cancer: fluorescence methodology for comparative semi-quantitative analysis

Katherine Ververis[1,2], Tom C Karagiannis[1,2]

[1]Epigenomic Medicine, Baker IDI Heart and Diabetes Institute, The Alfred Medical Research and Education Precinct, Melbourne, Victoria, Australia; [2]Department of Pathology, The University of Melbourne, Parkville, Victoria, Australia

Received December 7, 2011; accepted December 28, 2011; Epub January 5, 2012; Published January 15, 2012

Abstract: The histone deacetylase inhibitors, suberoylanilide hydroxamic acid (Vorinostat, Zolinza™) and depsipeptide (Romidepsin, Istodax™) have been approved by the US Food and Drug Administration for the treatment of refractory cutaneous T-cell lymphoma. Numerous histone deacetylase inhibitors are currently undergoing clinical trials, predominantly in combination with other cancer modalities, for the treatment of various haematological and solid malignancies. Most of the traditional compounds are known as broad-spectrum or pan-histone deacetylase inhibitors, possessing activity against a number of the 11 metal-dependent enzymes. One of the main questions in the field is whether class- or isoform-specific compounds would offer a therapeutic benefit compared to broad-spectrum inhibitors. Therefore, analysis of the relative expression of the different histone deacetylase enzymes in cancer cells and tissues is important to determine whether there are specific targets. We used a panel of antibodies directed against the 11 known mammalian histone deacetylases to determine expression levels in MCF7 breast cancer cells and in tissue representative of invasive ductal cell carcinoma and ductal carcinoma in situ. Firstly, we utilized a semi-quantitative method based on immunofluorescence staining to examine expression of the different histone deacetylases in MCF7 cells. Our findings indicate high expression levels of HDAC1, 3 and 6 in accordance with findings from others using RT-PCR and immunoblotting. Following validation of our approach we examined the expression of the different isoforms in representative control and breast cancer tissue. In general, our findings indicate higher expression of class I histone deacetylases compared to class II enzymes in breast cancer tissue. Analysis of individual cancer cells in the same tissue indicated marked heterogeneity in the expression of most class I enzymes indicating potential complications with the use of class- or isoform-specific compounds. Overall, our approach can be utilized to rapidly compare, in an unbiased semi-quantitative manner, the differential levels of expression of histone deacetylase enzymes in cells and tissues using widely available imaging software. It is anticipated that such analysis will become increasingly important as class- or isoform-specific histone deacetylase inhibitors become more readily available.

Keywords: Chromatin, histone acetylation, histone deacetylase inhibitor, breast cancer, immunofluorescence

Introduction

Acetylation is one of the most extensively researched post-translational modifications. It is mediated via the opposing actions of histone acetyltransferases (HATs) and histone deacetylases (HDACs) [1-3]. HATs catalyse the addition of an acetyl group to the ε-amino group of the lysine residue on the core histone tails [4]. This weakens the DNA-histone interaction resulting in a more relaxed, transcriptionally permissive, chromatin conformation [5-7]. Despite what their name suggests, HATs also catalyse the acetylation of non-histone proteins and are also referred to as K-acetyltransferases (KATs) [8]. HDACs catalyze the removal of acetyl groups from lysine residues resulting in a more condensed, transcriptionally repressive, chromatin structure [1]. Numerous non-histone substrates have also been identified for HDAC enzymes [9-12].

There are two distinct categories that classify the 18 mammalian HDACs. Firstly, the seven nicotinamide adenine dinucleotide (NAD^+)-dependent enzymes are known as the sirtuins

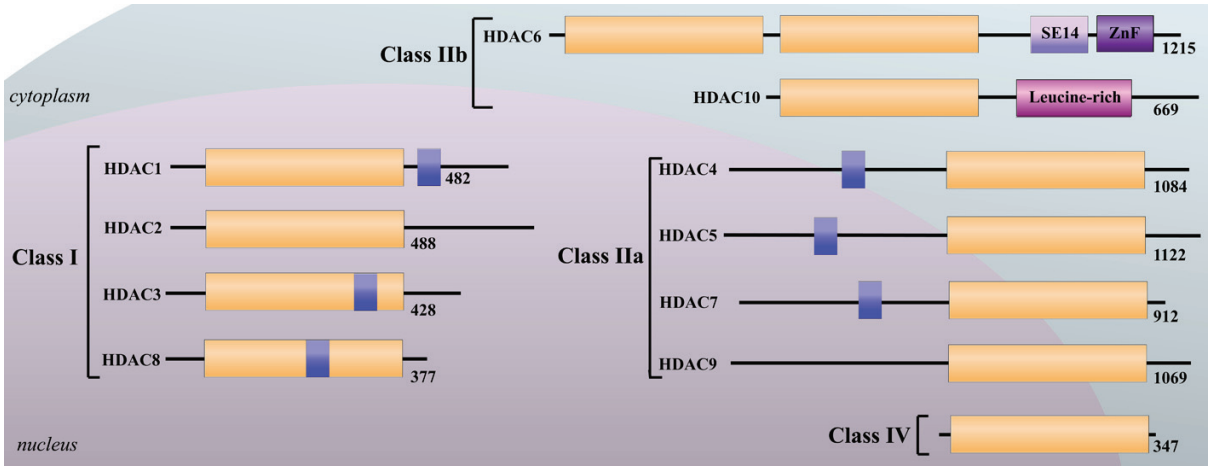

Figure 1. Classification of the classical histone deacetylases (HDACs). The classical HDACs are grouped into three classes based on their homology and sequence identity to yeast. They share a highly conserved deacetylase (DAC) domain shown as long orange cylinders. The class I HDACs (HDAC1, 2, 3 and 8) share homology to the yeast reduced potassium dependency-3 (Rpd-3) and are found primarily in the cell nucleus. Class II HDACs share sequence homology to the yeast histone deacetylase-1 (Hda1) and are sub-divided into two further classes; Class IIa (HDAC4, 5, 7 and 9) which shuttle between the cell cytoplasm and nucleus and Class IIb (HDAC6 and 10) which are found primarily in the cytoplasm. Class IV HDACs is comprised of HDAC11 which shares sequence homology to both Rpd-3 and Hda-1. Shown as small blue cylinders are nuclear localization sites and C- and N- terminal tail are shown as thick black lines. Total numbers of amino acid residues are shown at the N-terminal of each enzyme. SE14, Ser-Glu-containing repeats; ZnF, ubiquitin-binding zinc finger; Leucine-rich domain.

(SIRT1-7). These represent class III and are structurally homologous to the yeast silent information regulator 2 [13-15]. The second group are the 11 zinc-dependent enzymes which are known as the classical metal-dependent HDAC family and are the focus of this paper (**Figure 1**). The classical HDACs are divided into class I, II and IV and although they share a highly conserved catalytic deacetylase domain they differ in their N- and C- terminal tails, cellular localization and biological roles (**Figure 1**) [16]. Class I consists of HDAC1, 2, 3 and 8 and shares homology to the yeast reduced dependency 3 (RDP3) [17, 18]. These HDACs are primarily found in the nucleus and play a primary role in proliferation and cell survival [19]. Class II HDACs share homology to the yeast histone deacetylase-1 (Hda1) and includes the class IIa HDAC4, 5, 7 and 9 and class IIb HDAC6 and 10 [20, 21]. Class IIa HDACs shuttle between the nucleus and the cytoplasm and have tissue specific functions [11, 12, 17, 22-26]. Class IIb HDACs have two catalytic domains and are predominantly cytoplasmic. HDAC6 is unique as it contains an ubiquitin binding site and is a specific deacetylase of numerous non-histone substrates including: cell motility mediators, α-tubulin and cortactin; chaperones, HSP90 and HSP70; DNA repair proteins, Ku70 and signalling mediators such as β-catenin [27-29]. HDAC11 shares homology to both class I and II enzymes and represent class IV HDACs [16].

HDACs have direct and indirect affects in a plethora of cell pathways including cell cycle arrest, apoptosis, migration and cell senescence [25]. Therefore, there is great interest in the use of HDAC inhibitors as anti-cancer agents. Indeed, two HDAC inhibitors, suberoylanilide hydroxamine acid (SAHA; Vorinostat™) and depsipeptide (Romidepsin, Istodax™) have been approved by the US Food and Drug Administration (FDA) for the treatment of refractory cutaneous T-cell lymphoma [30, 31]. The two approved compounds and many of the HDAC inhibitors currently in clinical trials are referred to as broad-spectrum inhibitors as they inhibit multiple HDAC enzymes. There is emerging interest in the field regarding the potential use of class-specific or isoform-specific inhibitors in cancer. The argument is that they may be more beneficial in targeting malignant cells while minimizing aberrant effects on normal cell lines thereby providing a distinct therapeutic

advantage. However, the alternative argument is that the pleiotropic effects of broad-spectrum inhibitors may be advantageous given the heterogeneous nature of many cancers.

With respect to the clinical applicability of HDAC inhibitors and potential of more specific compounds, the expression HDACs in cancer is an important issue. Accumulating evidence suggests that class I HDACs are overexpressed in cancer tissues [32]. For example, several studies have highlighted the role of class I HDACs in breast cancer cells and tissues, many focusing on HDAC1, 3 and 6 [33-41]. The aim of this study was determine the expression the 11 classical metal-dependent mammalian HDACs in the epithelial breast cancer MCF7 cell line. In addition, we used representative ductal carcinoma in situ and invasive ductal carcinoma breast tissue in comparison to normal breast tissue to compare the expression of the classical HDACs in specific cell types. We validated an immunofluorescence approach which provides an unbiased, semi-quantitative comparison of the expression levels of the different HDAC enzymes in cells and tissues.

Materials and methods

Cell culture

Human breast adenocarcinoma MCF7 cells and epidermoid carcinoma A431 cells were obtained from the American Type Culture (Manassas, VA, USA). Cells were maintained in α-MEM medium supplemented with 2 mM L-glutamine, 10% fetal bovine serum and 80 μg/mL gentamicin. Cells were incubated in a humidified atmosphere containing 5% CO_2 at 37°C.

Breast tissue and histology

Control and breast cancer tissues were obtained from The University of Melbourne (Department of Anatomy and Cell Biology, Parkville, Australia) teaching archives. Histological observations were made using haematoxylin and eosin stained tissue sections. Images were acquired using an Olympus FSX100 Bio Imaging Navigator.

Immunofluorescence staining (cell studies)

Cells were plated in 8 well chamber sides (Nalge Nunc International, NY, USA) at densities of 25,000 cells/well. After 24 hours cells were fixed for 10 minutes using 4% paraformaldehyde (Sigma-Aldrich, St Louis, USA). After a 5 minute wash with phosphate buffered saline without calcium and magnesium (PBS), cells were permeabilized using 0.1% Triton X-100 (Sigma) for 10 minutes. After three consecutive washes with PBS, cells were blocked in 1% BSA for 20 minutes prior to incubation with primary antibody; polyclonal rabbit anti-HDAC1-11 (K333-11-30; Biovision, Mountain View, CA, USA) at a concentration of 10 μg/ml and in separate experiments monoclonal rabbit anti-phospho-EGFr (pT693) (2343-1; Epitomics, Burlingame, CA, USA) or polyclonal rabbit anti-phosho-EGFr (s695) (T3868; Epitomics) with polyclonal goat anti-beta actin (ab8229; Abcam, Cambridge, UK) diluted to 5μg/ml. Primary antibodies were incubated in a dark humidified environment overnight at 4°C. Following three consecutive washes, cells were incubated with a secondary donkey anti-goat antibody (1:500 in 1% BSA) conjugated with Alexa-488 (Molecular Probes, Oregon, USA) or Alexa-546 conjugated goat anti-rabbit secondary antibodies (at 1:500 dilution) (Invitrogen, Molecular Probes, Eugene, OR, USA) and incubated for 45 minutes in a dark humidified environment on a rotating platform at room temperature. Following three consecutive washes, cells were mounted with prolong Gold antifade solution containing DAPI (Invitrogen), coverslipped (Biolab, VIC, AUS) and sealed with nail varnish. Slides were incubated overnight at 4°C before imaging.

Immunofluorescence staining (tissue sections)

Paraffin embedded tissue was sectioned at a thickness of 5 microns. To dewax, tissue was incubated in xylene for 5 minutes, followed by incubation in fresh xylene for 1 minute and rehydrated in three consecutive incubations in ethanol each for 1 minute at 100%, 90% and 70%.

Tissue section were incubated in DAKO® Target Retrieval Solution (S1699; Thermo Scientific) at 1:10 dilution for 10 minutes in a pre-heated water bath at 95-99°C for activation of epitopes. Tissue sections were then removed from the water bath and allowed to cool for 20 minutes prior to decanting the target retrieval solution. Tissue sections were then permeabilized

with 0.1% Triton X-100 for 10 minutes followed by equilibration in 0.1% Tween 20 in two consecutive 15 minutes incubations. Tissue sections were outlined using a pap pen and blocked for 1 hour in Superblock (Thermo Scientific) followed by an overnight incubation in a humidified chamber with primary antibodies diluted in 1% BSA: polyclonal rabbit anti-HDAC1-11 (K333-11-30; Biovision) at a concentration of 10 μg/ml, monoclonal rabbit anti-HDAC4 (1576-1;Epitomics) diluted 1:500 and monoclonal mouse anti-HDAC8 (H6412; Sigma) diluted (1:500); polyclonal goat anti-beta actin (ab8229; Abcam) diluted to 5 μg/ml; monoclonal rabbit anti-Annexin V (2792-1; Epitomics); monoclonal rabbit anti-phospho-EGFr (pT693) (2343-1; Epitomics); polyclonal rabbit anti-phosho-EGFr (s695) (T3868; Epitomics) and monoclonal rabbit anti-CD71 (TFRC) (2918-1; Epitomics). After three washes in 0.1% Tween 20, 1% BSA in PBS, tissue was incubated in secondary antibodies diluted in 1% BSA for 1 hour with: goat anti-rabbit Alexa 546, goat anti-mouse Alexa 546 and donkey anti-goat Alexa 488 all at a dilution of 1:500 (Invitrogen) in a dark humidified chamber. Following three washes in 0.1% Tween 20, 1% BSA in PBS, tissues were mounted in Prolong Gold Antifade mounting medium containing DAPI (Invitrogen) and sealed with nail varnish. Slides were incubated overnight at 4°C before imaging.

Image acquisition and analysis

Images were acquired using an Olympus BX61 motorised upright fluorescence microscope automated with FVII Camera using a 10x/0.3 and 20x/0.5 Uplan FL objectives. Fluorescence filter cubes used included: DAPI (Ex: 350/50, Em: 460/50nm), FITC (Ex: 470/40, Em: 525/50nm) and TRITC (Ex:545/30, Em:620/60nm). Semi-quantitative analysis of the relative HDAC expression intensity was examined and scored by three individuals independently on a scale of low to high (0-5) intensity for a minimum of five breast regions. Global expression levels were calculated as the sum of regional expression values and an overall rank order of expression was generated. Semi-quantitative analysis of relative HDAC intensity was performed using Fiji software (Image J). Colour images were separated and red channel images were measured for mean fluorescence intensity. Mean intensity was determined from a minimum of 100 cells for each HDAC enzyme.

Western blotting

MCF7 and A431 cells were harvested by trypzinisation and washed in ice-cold PBS. Whole cell lysates were extracted using Mammalian Protein Extraction Reagent (M-PER; Thermo Scientific, Rockford, USA) and total protein was measured using the Bradford assay with bovine serum albumin (BSA; Sigma) at 595nM using an Emax Precision microplate reader. Equal amounts of protein (40 μg/lane) were fractionated using 4-12% Bis-Tris (NP0335; Invitrogen) SDS-PAGE and transferred to nitrocellulose membranes. The membranes were incubated overnight with primary antibodies: polyclonal rabbit anti-HDAC (2 μg/ml; K333-11-30; Biovision), monoclonal rabbit anti-HDAC4 (1:10000; 1576-1, Epitomics), monoclonal mouse anti-HDAC8 (1:10000; H6412, Sigma) and rabbit monoclonal anti-HDAC6 (1:15000; EPR6160, Epitomics). The membranes were incubated with peroxidise-conjugated goat anti-mouse or donkey anti-rabbit secondary antibodies (1:10000) followed by enhanced chemilluminescence (ECL-CPS3500-1KT, Sigma) staining.

Statistical analysis

A minimum of 7 breast lobules were analysed in the control breast and a minimum of 5 breast regions on the cancer breast. A minimum of two independent experiments were completed for all cell-based assays. Results are expressed as the mean ± standard deviation (SD). Statistical analysis was performed using a one-way analysis of variance with a Bonferroni post test using GraphPad Prism (version 5). *P<0.05, **P<0.01, ***P<0.001.

Results and discussion

Expression of HDAC enzymes in MCF7 and A431 cells

We investigated the expression of the metal-dependent HDAC enzymes in the both the nucleus and cytoplasm of the adenocarcinoma breast epithelial MCF7 cell line by immunofluorescence. The fluorescence was firstly analyzed by observation by scoring expression from 0-5 (low-high). The mean results of three independent experiments are shown in **Table 1**. We repeated the analysis using Image J software to measure the mean fluorescence intensity in

Table 1. Semi-quantitative analysis of HDAC expression in MCF7 and A431 (Observational analysis)

	HDAC		MCF7	TOTAL SUM	RANK	A431	TOTAL SUM	RANK
Class I	HDAC1	nuc	2.51 ± 1.0	4.34	2	1.06 ± 1.5	2.33	10
		cyt	1.83 ± 0.9			1.27 ± 0.1		
	HDAC2	nuc	2.72 ± 0.6	3.69	7	1.67 ± 2.4	3.08	9
		cyt	1.28 ± 0.3			1.42 ± 1.1		
	HDAC3	nuc	3.22 ± 0.3	5.56	1	2.42 ± 0.8	5.25	4
		cyt	2.34 ± 1.2			2.83 ± 1.9		
	HDAC8	nuc	1.21 ± 1.0	3.04	9	1.25 ± 1.1	4.33	7
		cyt	1.83 ± 1.6			3.08 ± 2.0		
Class IIa	HDAC4	nuc	3.03 ± 0.2	3.86	5	3.17 ± 0.5	7.00	1
		cyt	0.83 ± 0.1			3.82 ± 1.2		
	HDAC5	nuc	1.79 ± 1.1	3.92	4	1.58 ± 0.1	3.83	8
		cyt	2.13 ± 1.1			2.25 ± 2.0		
	HDAC7	nuc	0.2 ± 0.0	2.03	6	2.67 ± 2.4	6.33	2
		cyt	1.83 ± 0.0			3.67 ± 0.0		
	HDAC9	nuc	2.21 ± 1.1	3.39	8	0.33 ± 0.2	0.83	11
		cyt	1.18 ± 1.0			0.50 ± 0.7		
Class IIb	HDAC6	nuc	1.26 ± 1.4	4.01	3	2.08 ± 2.9	5.00	5
		cyt	2.75 ± 0.4			2.93 ± 0.6		
	HDAC10	nuc	1.23 ± 1.5	2.29	10	1.42 ± 1.8	4.50	6
		cyt	1.06 ± 0.3			3.08 ± 0.8		
Class IV	HDAC11	nuc	0.75 ± 0.4	1.67	11	2.00 ± 0.9	5.33	3
		cyt	0.92 ± 0.4			3.33 ± 0.9		

both the nucleus and cytoplasm of a minimum of 100 cells (**Table 2**). We performed the experiments and analysis in parallel using the epidermoid carcinoma, A431 cell line which is positive for all HDAC enzymes, as a control. We found HDAC1, 3 and 6 to be the most highly expressed HDAC enzymes in the MCF7 cells. Expression of the class I HDACs was not found to be localised exclusively in the nucleus but was also found to a lesser extent in the cytoplasm of the cells. HDAC6 and 10 were also not found to be primarily in the cytoplasm but were also observed in the nucleus of the cells. Comparatively, class II enzymes were generally expressed to a greater extent in A431 cells compared to class I HDACs (**Table 1**). We found our results to be consistent with those analysed using Image J (**Figure 2**) with only small deviations (less than 2) in rank order in comparison to our observational findings (**Table 2**).

We validated our findings of HDAC expression by immunobloting with selected anti-HDAC antibodies in both MCF7 and A431 cells (**Figure 2C**). We further confirmed our results using different primary antibodies representative from class I, class IIa and class IIb by immunoblots of rabbit anti-HDAC4 (Epitomics), rabbit anti-HDAC6 (Epitomics) and mouse anti-HDAC8 (Sigma). The results were similar to those with the anti-HDAC1-11 kit (Biovision). Finally we explored the expression of two cell surface receptors (as controls), the epidermal growth factor receptor (EGFr) and the transferrin receptor (CD71). Upregulation of the EGFR signalling has been correlated in a wide variety of tumours with progression to invasion and metastasis [42]. We found weak staining of the EGFr isoform pT693 in MCF7 cells in comparison to the strong staining observed in A431 cells (**Figure 3A** and **3B**), a cell line known to have high expression of the receptor [43]. Similar staining of the EGFr isoform s695 was observed in both MCF7 and A431 cells (**Figure 3C** and **3D**). Alternatively, we found weak to no staining of the transferrin receptor (CD71) on both MCF7 and A431 cells (**Figure 3E** and **3F**). Previous studies have used RT-PCR and Western blotting to determine mRNA and protein expression of HDACs and found HDAC1, 3 and 6 to be strongly expressed in estrogen receptor (ER) α and progesterone (PR) positive MCF7 cells and HDAC2, 4 and 8 to be expressed to a lesser extent [39, 41, 44]. Further, it has been found that expression of HDACs 1-3 is elevated in the breast cancer cell lines, SKBr3, MDA-MB-468, MCF7, MDA-MB-435, BT-20 and MDA-MB-231 [45]. These observations are in accordance with our im-

Table 2. Semi-quantitative analysis of HDAC expression in MCF7 and A431 (Image J analysis)

	HDAC		MCF7	TOTAL SUM	RANK	A431	TOTAL SUM	RANK
Class I	HDAC1	nuc	125.78 ± 15.9	223.35	1	47.21 ± 8.5	77.85	7
		cyt	97.56 ± 19.1			30.64 ± 22.1		
	HDAC2	nuc	88.47 ± 42.1	149.73	5	36.42 ± 0.5	56.87	10
		cyt	61.26 ± 23.9			20.44 ± 3.6		
	HDAC3	nuc	132.81 ± 30.1	194.11	2	90.78 ± 17.9	150.3	2
		cyt	61.30 ± 15.5			59.6 ± 10.9	1	
	HDAC8	nuc	74.48 ± 5.4	142.88	6	54.11 ± 18.0	95.12	4
		cyt	68.40 ± 4.0			41.0 ± 10.5		
Class IIa	HDAC4	nuc	123.88 ± 15.0	188.30	3	112.81 ± 11.8	177.2	1
		cyt	64.42 ± 22.2			64.39 ± 6.3	0	
	HDAC5	nuc	82.45 ± 43.6	157.19	4	75.84 ± 37.9	148.3	3
		cyt	74.73 ± 45.3			72.55 ± 15.3	9	
	HDAC7	nuc	48.12 ± 21.3	108.21	8	44.93 ± 23.9	87.15	5
		cyt	60.09 ± 19.7			42.22 ± 12.2		
	HDAC9	nuc	67.69 ± 17.4	106.37	10	26.63 ± 5.5	55.38	11
		cyt	38.81 ± 10.9			28.75 ± 0.8		
Class IIb	HDAC6	nuc	60.67 ± 18.5	112.44	7	25.07 ± 2.1	58.20	9
		cyt	51.77 ± 8.5			33.13 ± 5.4		
	HDAC10	nuc	43.99 ± 9.7	107.35	9	32.07 ± 1.9	77.70	8
		cyt	63.36 ± 20.6			45.63 ± 4.1		
Class IV	HDAC11	nuc	59.27 ± 6.9	100.14	11	46.23 ± 3.7	86.64	6
		cyt	40.56 ± 3.4			40.36 ± 8.0		

munofluorescence findings.

Histological examination of breast tissue

The breast is composed of specialized epithelium and stroma that give rise to both benign and malignant lesions specific to the organ. Between six to 12 lobules, comprising of the major ductal systems originate at the nipple. The squamous epithelium of the overlying skin continues into the ducts at the nipple and abruptly changes into a double-layered cuboidal epithelium. Each of the major lobules continues to have successive branching leading to terminal duct lobular units (TDLU) where successive branching in the TDLU arises to form clusters of ductules or acini in a lactating woman (**Figure 4Ai**). Ducts and lobules are lined by two cell types: a low flattened discontinuous layer of contractile cells containing myofilaments; myoepithelial cells and are found on the basement membrane. The luminal cells of the lobules are columnar epithelial cells and apocrine cells in the terminal ducts and ductules producing milk but not in main ducts of the lobules (**Figure 4A**). Our normal tissue represents active breast tissue given the approximate 50:50 ratio of ductules to stroma. Surrounding the lobules is the interlobular stroma which is made up of dense fibrous connective tissue with adipose tissue (**Figure 4Aiv**). Enclosing the lobules, the intralobular stroma is a hormonally responsive, delicate connective tissue which is specific to the breast and contains a scattering of lymphocytes (**Figure 4Aii**).

Breast cancer most often originates in the lobules or in the ducts of the breast. Malignant disease that originates in a lobule or duct is an "in situ" cancer (**Figure 4Bi**) as long as it does not penetrate through the basement membrane. The basement membrane lining each acinus is an important strong barrier that is not easily breached. Only aggressive cancers are able to breach the basement membrane and are named invasive breast carcinoma (**Figure 4Bii**). Here we have breast tissue with regions of both ductal carcinoma in situ (DCIS) and invasive ductal carcinoma.

In invasive or infiltrating ductal carcinoma we observe regions of abnormal proliferation of the epithelium of the ducts and invasion into the stroma were duct and stroma are no longer distinctly visible forming neoplasms or solid masses. Invasive carcinomas are the most common lesions detected as densities as can be observed as a large or solid collection or mass (**Figure 4Bi**). In other areas calcification associated with secretory material can be observed as

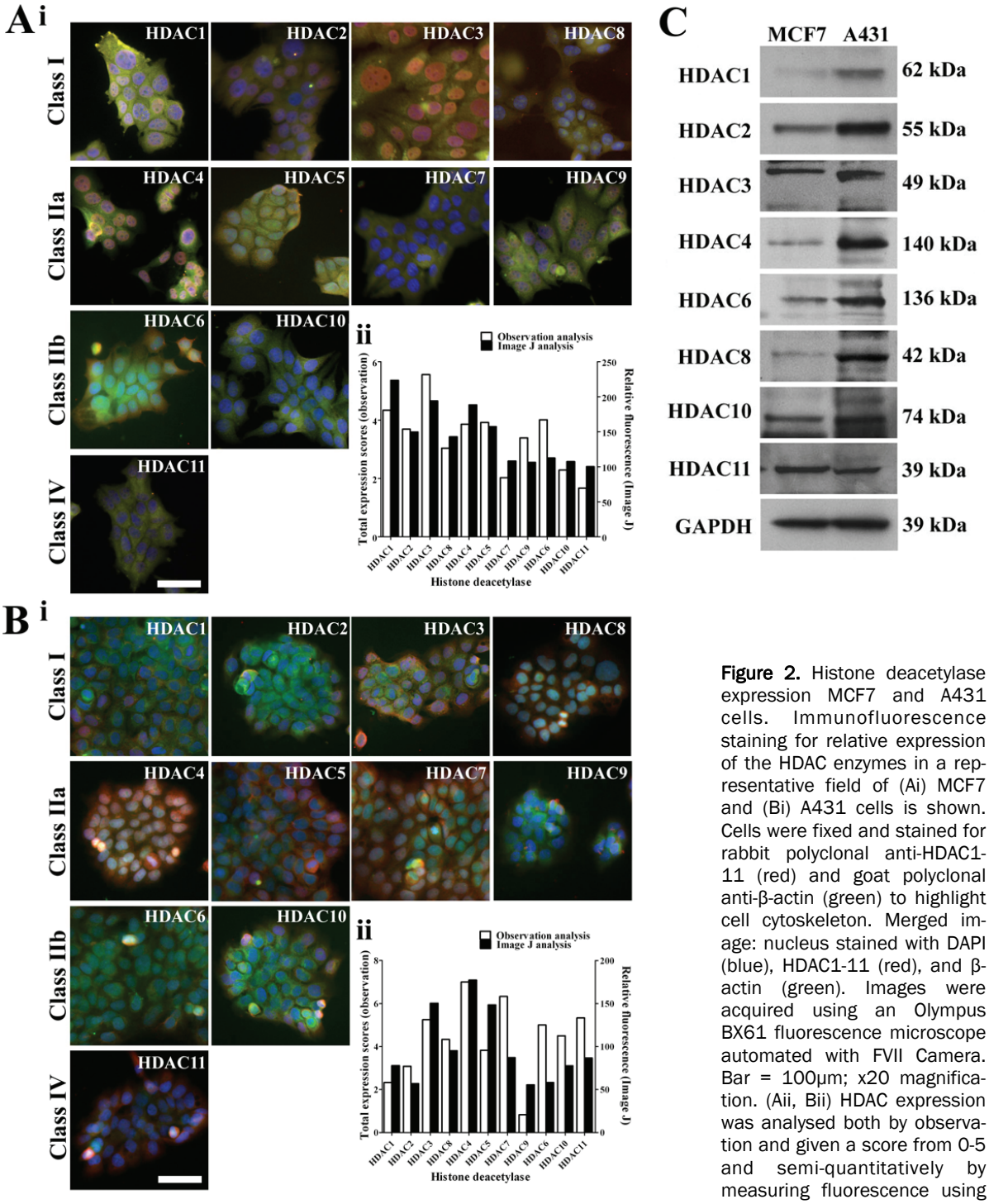

Figure 2. Histone deacetylase expression MCF7 and A431 cells. Immunofluorescence staining for relative expression of the HDAC enzymes in a representative field of (Ai) MCF7 and (Bi) A431 cells is shown. Cells were fixed and stained for rabbit polyclonal anti-HDAC1-11 (red) and goat polyclonal anti-β-actin (green) to highlight cell cytoskeleton. Merged image: nucleus stained with DAPI (blue), HDAC1-11 (red), and β-actin (green). Images were acquired using an Olympus BX61 fluorescence microscope automated with FVII Camera. Bar = 100μm; x20 magnification. (Aii, Bii) HDAC expression was analysed both by observation and given a score from 0-5 and semi-quantitatively by measuring fluorescence using Image J. Shown is the sum of the total fluorescence in the nucleus and cytoplasm measured by both methods. Relatively, strong staining was observed for HDAC1, 6 and 8 in MCF7 cells and HDAC4 and 7 in A431 cells. (C) Equal amounts of MCF7 and A431 cells (40 μg/lane) of whole-cell lysates were fractionated on SDS -PAGE gels, transferred to nitrocellulose membranes and immunoblotted for the indicated HDACs. GAPDH protein was blotted as a loading control.

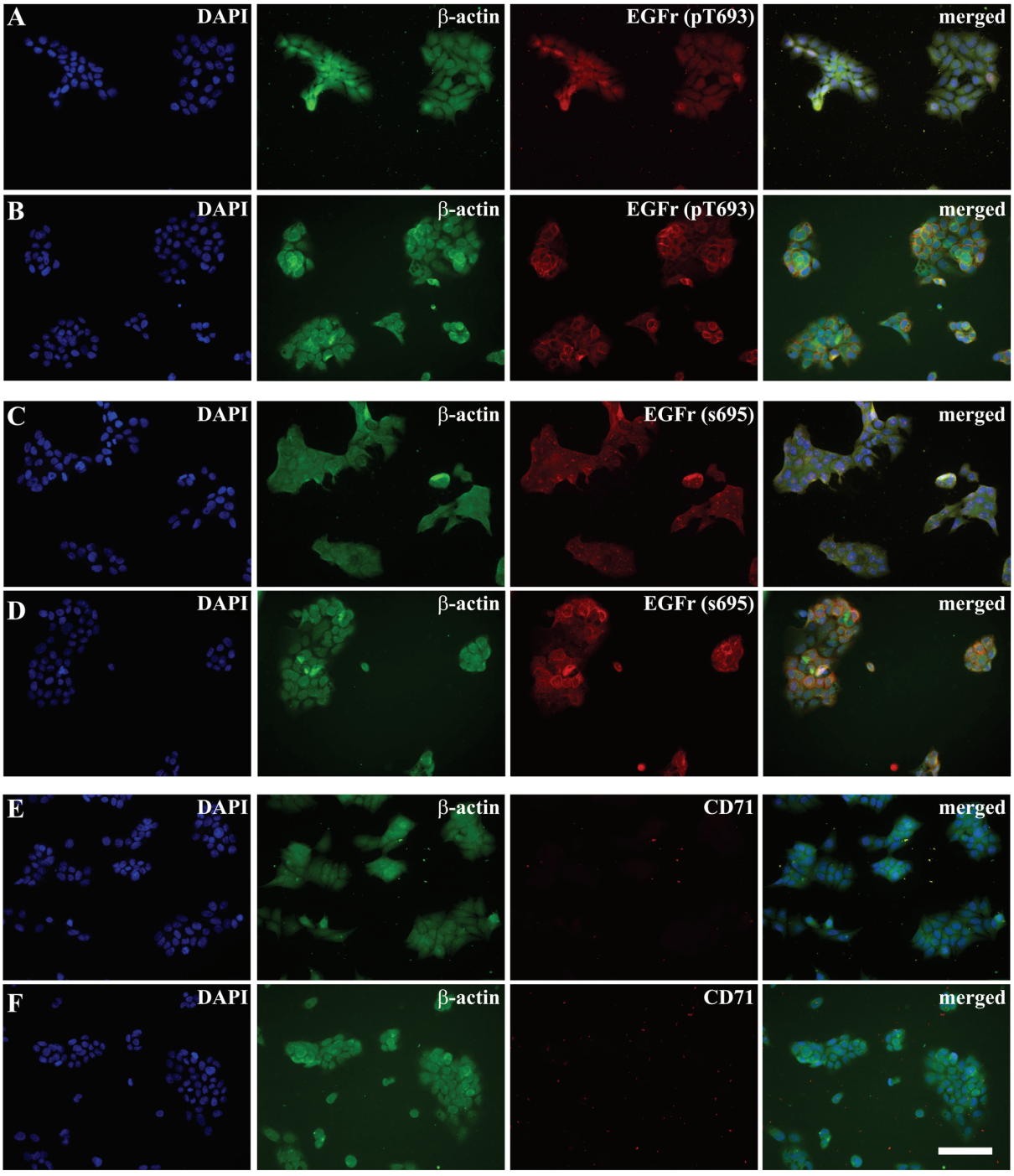

Figure 3. Distribution epidermal growth factor (EGFr) and transferrin receptors. MCF7 and A431 cells were stained with monoclonal rabbit anti-phospho-EGFr (pT693); polyclonal rabbit anti-phosho-EGFr (s695) and monoclonal rabbit anti-CD71 (TFRC) antibodies. (A) Non specific background staining of EGF receptor phosphorylated on threonine 693 (pT693) was observed in MCF7 cell in contrast to (B) strong positive staining observed A431 cells. (C) Medium staining of EGF receptor phosphorylated on serine 695 (s695) was observed in MCF7 cells in contrast to (D) strong staining observed in A431 cells. Transferrin receptor (red) was found to be negative in both (E) MCF7 and (F) A431 cells. Merged image: nucleus stained with DAPI (blue), EGFr and CD71 (red), β-actin (green). Images were acquired using an Olympus BX61 fluorescence microscope with automated FVII camera. Bar = 200μm x20 magnification.

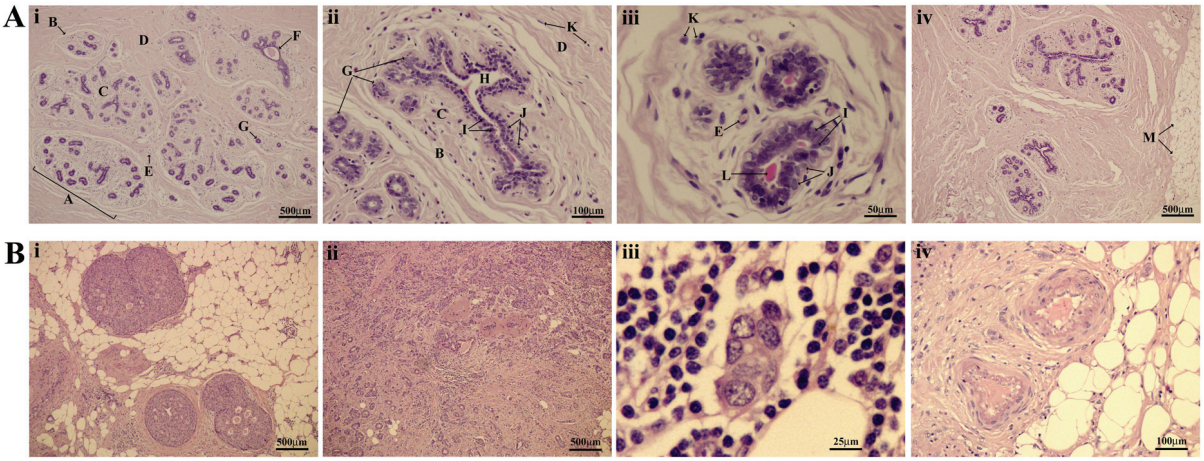

Figure 4. Histological representation of the morphological changes of breast tissue in cancer. Representative photomicrographs of haematoxylin and eosin stained sections of an active breast (a) and invasive ductal carcinoma (b). (i) Lobules of the breast arise from the lactiferous duct and through successive branching diminishing in size to form the terminal duct lobular unit (TDLU) (A). (ii) The TDLU is a continuation of the interlobular ducts (F) lumen (H) and end protruding into blunt or round saccules called ductules (G). Each TDLU is embedded in specialized hormonally responsive dense connective tissue called the intralobular stroma (C). The perimeter of the TDLU is surrounded by loose connective tissue (B) and is separated by dense interlobular connective tissue called stroma (D) which contains fibroblasts (K). Blood vessels (E) circulate throughout the intralobular stroma and interlobular stroma. (iii) During lactation, the ductules differentiate into the secretory units called acini, producing milk (L). Each ductules or acini are lined with cuboidal epithelium (I) and an outer layer of myoepithelium (J). (iv) Adipose tissue is found surrounding TDLUs, (M) highlighting were adipocytes are found. (b) Breast tissue with regions of both ductal carcinoma 'in situ' and invasive ductal carcinoma. (i) representative image of ductal carconima 'in situ' with small irregular clusters of calcifications of secretory material within the lumens of the duct. (ii) infiltrating ductal carcinoma cells originating from the ducts invade the stroma. (iii) A magnified region showing intraductal inflammation. (iv) Evidence of radial scarring shown by stallate lesions of trapped ductal cells in hyalinised stroma. Images were acquired using an Olympus FSX100 microscope. Bar = 500μm, 100μm, 50μm, 25μm; x4, x20, x40, x80 magnification, respectively.

small irregular clusters in invasive carcinomas and most likely apocrine cysts, these are present within the lumen of the ductules (**Figure 4Bii, 4Biii**). In other regions, we observed stromal fibrosis completely compress the lumens of ductules to create the appearance of solids cords or double strands of cells lying within dense stroma. There is also evidence of radial scars shown by the stellate lesions characterized by trapped glands encapsulated by hyalinised stroma (**Figure 4Biv**).

Expression of HDAC enzymes in control and breast cancer

To examine HDAC expression in control (**Figure 5**) and breast tissue (**Figure 6**), we used immunofluorescence assays. Class I HDAC enzymes were found to be only minimally expressed throughout all cell types in the control breast tissue with all cell types scoring below 1.2 and expression was localized predominantly in the nucleus. Of the Class I HDAC enzymes, HDAC8 was found to be expressed the highest in both the luminal cuboidal epithelium and myoepithelium. Endothelial cells appeared to have no expression of both HDAC1 and HDAC2 and fibroblast cells also appeared to be negative for HDAC1 expression (**Table 3**).

In contrast, class I HDAC enzymes: HDACs 2, 3 and 8 were significantly elevated in breast cancer tissue and found to be ranked the overall three highest expressing HDAC enzymes (**Figure 7**). HDAC2, 3 and 8 expression was observed to be primarily elevated in nucleus of the ductal carcinoma cells, however expression was also observed in the cytoplasm of these cells. In addition, the heterogeneity of inflammatory cells was most obvious with HDACs 2, 3 and 8. Inflammatory cells could be divided into two distinct groups: one which were observed to have little or no HDAC staining and the other which had medium to high levels of staining. This ob-

Table 3. Semi-quantitative analysis of HDAC expression in control breast tissue*

Class	HDAC		luminal cuboidal epithelium	myoepithelium	microvascular endothelial cells	fibro-blasts	SUM	TOTAL SUM	RANK
Class I	HDAC1	nuc	0.6 ± 0.5	0.3 ± 0.5	0.0 ± 0.0	0.0 ± 0.0	0.9	0.9	9
		cyt	0.0 ± 0.0	0.0 ± 0.0	0.0 ± 0.0	0.0 ± 0.0	0		
	HDAC2	nuc	1.0 ± 0.6	0.5 ± 0.5	0.0 ± 0.0	0.2 ± 0.4	1.7	1.7	8
		cyt	0.0 ± 0.0	0.0 ± 0.0	0.0 ± 0.0	0.0 ± 0.0	0		
	HDAC3	nuc	0.3 ± 0.5	0.3 ± 0.5	0.2 ± 0.4	0.3 ± 0.8	1.1	1.1	9
		cyt	0.0 ± 0.0	0.0 ± 0.0	0.0 ± 0.0	0.0 ± 0.0	0		
	HDAC8	nuc	0.7 ± 0.5	0.7 ± 0.5	0.8 ± 0.8	1.2 ± 0.8	3.4	3.4	6
		cyt	0.0 ± 0.0	0.0 ± 0.0	0.0 ± 0.0	0.0 ± 0.0	0		
	HDAC8 (Sigma)	nuc	1.0 ± 0.0	1.0 ± 0.0	0.3 ± 0.6	0.7 ± 0.6	3	3	
		cyt	0.0 ± 0.0	0.0 ± 0.0	0.0 ± 0.0	0.0 ± 0.0	0		
Class IIa	HDAC4	nuc	2.0 ± 0.4	3.0 ± 0.5	3.0 ± 0.5	1.0 ± 0.5	9	18.5	1
		cyt	3.0 ± 0.0	2.0 ± 0.5	3.0 ± 1.0	1.5 ± 1.2	9.5		
	HDAC4 (Epitomics)	nuc	2.0 ± 0.0	3.0 ± 0.6	3.0 ± 0.0	1.0 ± 0.6	9	18.5	
		cyt	3.0 ± 0.6	2.0 ± 0.6	3.0 ± 1.2	1.5 ± 0.2	9.5		
	HDAC5	nuc	3.1 ± 0.9	2.7 ± 0.8	0.7 ± 1.1	1.1 ± 0.9	7.6	16.3	2
		cyt	3.0 ± 1.3	2.0 ± 1.0	0.4 ± 0.5	3.3 ± 1.0	8.7		
	HDAC7	nuc	1.0 ± 0.0	1.3 ± 0.5	0.7 ± 0.5	0.8 ± 0.4	3.8	9.9	4
		cyt	2.0 ± 0.6	2.3 ± 0.5	1.0 ± 0.0	0.8 ± 0.4	6.1		
	HDAC9	nuc	4.6 ± 0.5	3.6 ± 0.5	0.4 ± 0.8	1.1 ± 1.5	9.7	16.7	3
		cyt	3.7 ± 0.5	1.1 ± 1.1	0.1± 0.4	2.1 ± 1.1	7		
Class IIb	HDAC6	nuc	0.4± 0.5	0.4 ± 0.5	0.3 ± 0.5	0.0 ± 0.0	1.1	5.8	5
		cyt	2.3 ± 1.1	0.9 ± 0.4	0.4 ± 1.1	1.1 ± 0.9	4.7		
	HDAC10	nuc	0.0 ± 0.0	0.0 ± 0.0	0.0 ± 0.0	0.0 ± 0.0	0	0.4	10
		cyt	0.0 ± 0.0	0.0 ± 0.0	0.0 ± 0.0	0.4 ± 1.1	0.4		
Class IV	HDAC11	nuc	0.1 ± 0.4	0.1 ± 0.4	0.0 ± 0.0	0.0 ± 0.0	0.2	0.2	11
		cyt	0.0 ± 0.0	0.0 ± 0.0	0.0 ± 0.0	0.0 ± 0.0	0		

*n = 7

servation was found to be exclusive to these three enzymes (**Table 4**).

In all of the cell types investigated in the control breast tissue (**Table 3**), the class II HDAC enzymes: HDACs 4, 5, 7 and 9 were found to be expressed in approximately equal amounts within the nucleus and cytoplasm. Overall medium staining was found for most HDAC enzymes in all cell types except for fibroblasts which expressed low amounts of each class II HDAC enzymes (between 0.8-3.3). HDAC9 was found to be expressed the highest in both the nucleus (4.6 ± 0.5) and cytoplasm (3.7 ± 0.5) of the luminal cuboidal epithelium in comparison to other HDAC enzymes. Overall the class II HDAC enzymes were observed to have the strongest staining in comparison to other HDACs (**Figure 5**) with HDACs 4, 5, 9 then 7 being ranked 1-4 respectively for overall expression.

In contrast, the breast cancer tissue showed an overall weak staining of class II HDAC enzymes in all cell types (**Figure 6**). This observation was significantly different to the staining observed in both the nucleus and cytoplasm of cells found in the normal breast tissue (**Figure 7**). HDAC7 was found to be highly expressed within the cytoplasm of the ductal carcinoma cells (4.1 ± 0.3) which was different to staining of both the carcinoma cells and inflammatory cells for the other class II HDACs which scored no greater than 1.8 (**Table 3**).

Only subtle differences were found in HDAC6 expression of the control breast tissue in comparison to the cancer tissue. It was primarily expressed in the cytoplasm of all cell types. HDAC10 and 11 was found to have little to no staining in the control breast tissue with overall sum of scores of 0.4 and 0.2 and ranked 10th and 11th, respectively (**Table 3**). Similarly, HDAC11 was not observed in the ductal carcinoma or inflammatory cells in the breast tissue; ranked 11th in the breast tissue. However, strong staining was observed in the cytoplasm of the ductal carcinoma cells scoring 3.9 ± 1.9 and weak staining was observed in the cytoplasm of the inflammatory cells scoring 1.3 ±

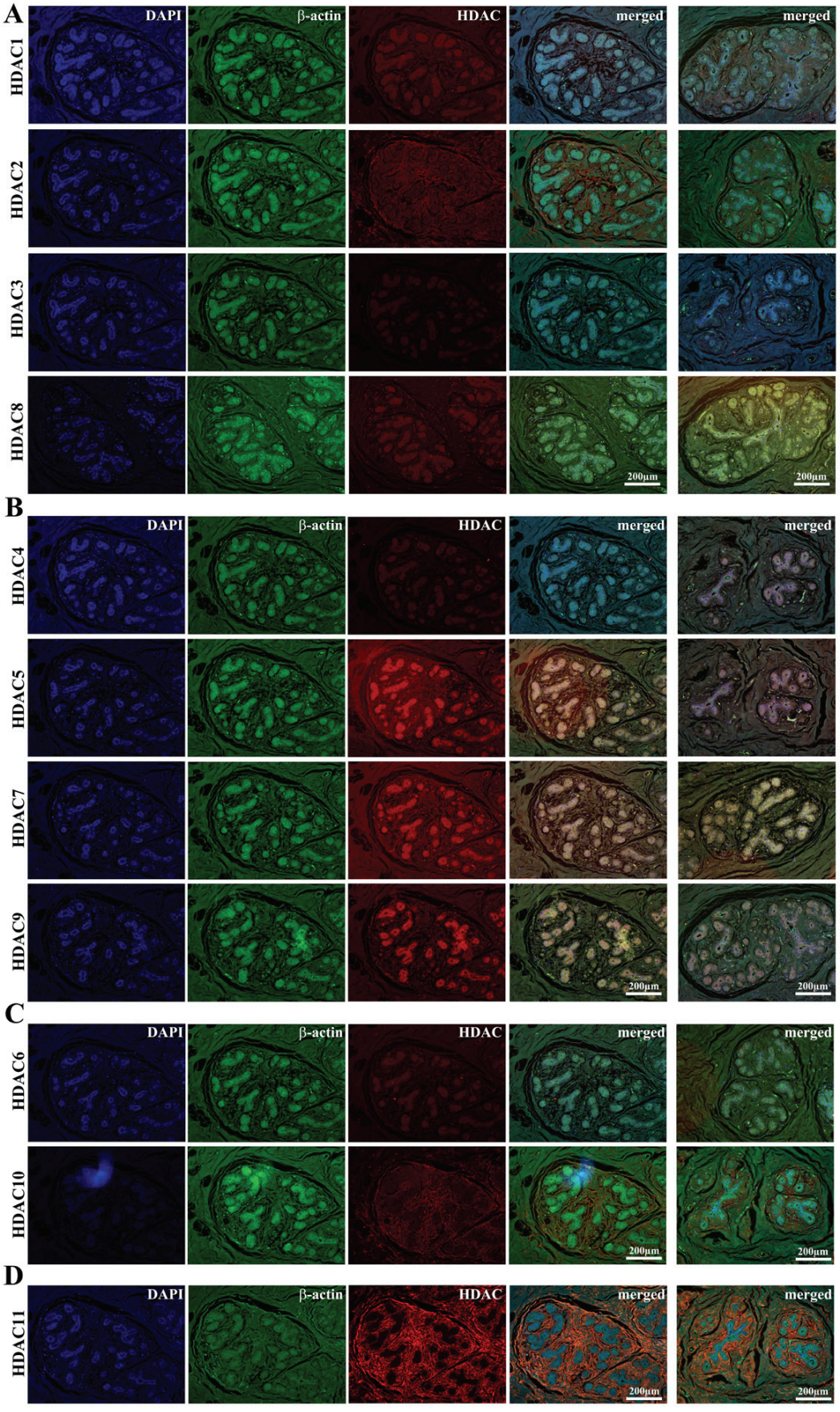
A
HDAC1
HDAC2
HDAC3
HDAC8
DAPI
β-actin
HDAC
merged
merged
200μm
B
HDAC4
HDAC5
HDAC7
HDAC9
C
HDAC6
HDAC10
D
HDAC11

Figure 5. Histone deacetylases expression in normal breast tissue. Immunofluorescence staining for relative expression of Class I HDACs (A), Class IIa HDACs (B), Class IIb HDACs (C) and Class IV HDACs (D) in two representative normal breast lobules. Paraffin embedded tissue sections were fixed and stained for rabbit polyclonal anti-HDAC1-11 (red) and goat polyclonal anti-β-actin (green) to highlight tissue structure. Weak staining was observed across Class I and Class IIb HDACs and strong staining was observed in class IIa HDACs. Strong non-specific staining of HDAC11 was seen in the connective tissue of the stroma with very weak staining seen in the actual cells. Show is an artefact for DAPI staining in the representative image of HDAC10 and for red channel in HDAC5. Merged image: nucleus stained with DAPI (blue), HDAC1-11 (red), and β-actin (green). Images were acquired using an Olympus BX61 fluorescence microscope automated with FVII Camera at x20 magnification. Bar = 200μm; x10 magnification.

Table 4. Semi-quantitative analysis of HDAC expression in invasive breast carcinoma tissue*

Class	HDAC		ductal carcinoma cells	inflammatory cells I	inflammatory cells II	SUM	TOTAL SUM	RANK
Class I	HDAC1	nuc	0.3 ± 0.5	0.5 ± 0.6		0.8	2.1	9
		cyt	0.8 ± 1.0	0.5 ± 0.6		1.3		
	HDAC2	nuc	4.4 ± 0.8	0.8 ± 1.5	3.0 ± 1.4	8.2	9.3	3
		cyt	0.8 ± 0.5	0.0 ± 0.0	0.3 ± 0.5	1.1		
	HDAC3	nuc	2.9 ± 1.0	0.8 ± 1.5	3.3 ± 0.6	7	14.7	2
		cyt	3.4 ± 1.6	2.0 ± 1.6	2.3 ± 1.5	7.7		
	HDAC8	nuc	2.8 ± 0.5	0.5 ± 1.0	2.5 ± 0.7	5.8	16.6	1
		cyt	4.8 ± 0.5	2.5 ± 1.7	3.5 ± 0.7	10.8		
	HDAC8 (Sigma)	nuc	2.5 ± 1.3	0.8 ± 0.0	2.0 ± 0.0	5.3	15.9	
		cyt	4.3 ± 1.0	3.3 ± 0.5	3.0 ± 0.0	10.6		
Class IIa	HDAC4	nuc	0.5 ± 1.5	0.3 ± 0.5		0.8	4.1	6
		cyt	1.5 ± 1.9	1.8 ± 1.0		3.3		
	HDAC4 (Epitomics)	nuc	0.3 ± 0.6	0.0 ± 0.0		0.3	2.7	
		cyt	1.7 ± 1.2	0.7 ± 0.6		2.4		
	HDAC5	nuc	0.3 ± 0.5	0.3 ± 0.5		0.6	2.9	8
		cyt	1.3 ± 0.8	1.0 ± 1.0		2.3		
	HDAC7	nuc	1.5 ± 0.6	0.5 ± 0.6		2	7.4	4
		cyt	4.1 ± 0.3	1.3 ± 0.5		5.4		
	HDAC9	nuc	1.4 ± 0.5	0.0 ± 0.0		1.4	3.7	7
		cyt	1.0 ± 0.0	1.3 ± 1.0		2.3		
Class IIb	HDAC6	nuc	1.5± 0.6	0.0 ± 0.0		1.5	2	10
		cyt	3.4 ± 0.8	1.6 ± 0.9		5		
	HDAC10	nuc	0.0 ± 0.0	0.0 ± 0.0		0	5.2	5
		cyt	3.9 ± 1.9	1.3 ± 1.5		5.2		
Class IV	HDAC11	nuc	0.0 ± 0.0	0.0 ± 0.0		0	0.3	11
		cyt	0.0 ± 0.0	0.3 ± 0.5		0.3		

*n = 5

1.5 (**Table 4**). We noted strong staining in the stroma for HDACs 2, 10 and 11 in the control breast tissue (**Figure 5**). This staining was not scored or taken into account in the overall expression scores as we believe it is non-specific collagen staining.

Our observations are in accordance with those of previous studies indicating overexpression of class I HDACs in breast cancer. For example, a study which examined the expression of class I HDACs in several cell lines and human cancer tissues including stomach, esophagus, colon, prostate, breast, ovary, lung, pancreas and thyroid cancer found that greater than 75% of the epithelial cells showed high expression of HDACs 1, 2, 3 and 8 in accordance with our findings [32]. However, there is marked heterogeneity between breast cancers and our study should be viewed predominantly as a methodology paper. For example, it has been shown that only 39.8% and 43.9% of breast cancers are positive for HDAC1 and HDAC3 respectively, and there was a direct correlation HDAC1 and 3 ex-

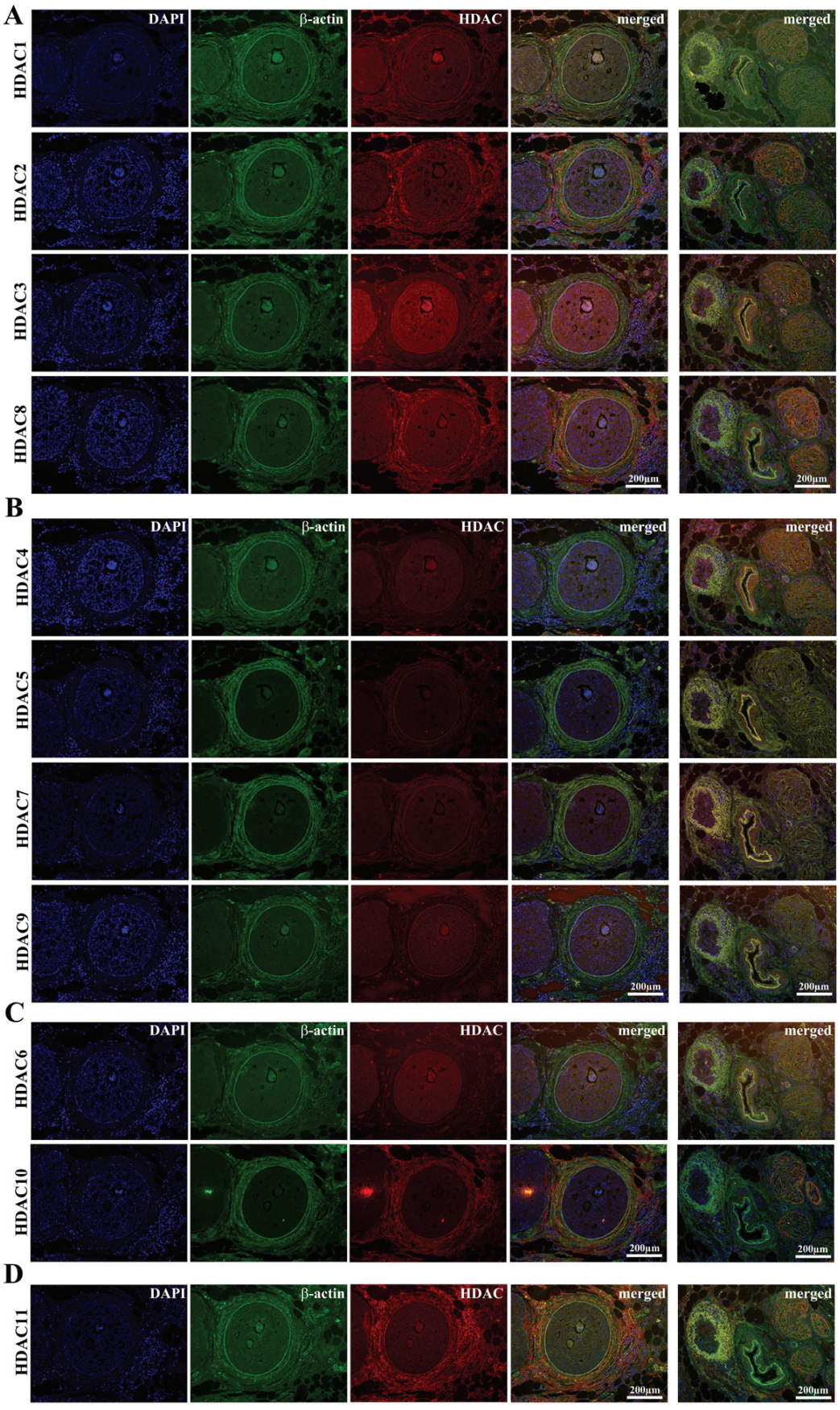
A
HDAC1
HDAC2
HDAC3
HDAC8
DAPI
β-actin
HDAC
merged
merged
200μm
B
HDAC4
HDAC5
HDAC7
HDAC9
C
HDAC6
HDAC10
D
HDAC11

Figure 6. Histone deacetylases HDAC expression in breast carcinoma. Immunofluorescence staining for relative expression of Class I HDACs (A), Class IIa HDACs (B), Class IIb HDACs (C) and Class IV HDACs (D) in two representative fields of breast carcinoma. Paraffin embedded tissue sections were fixed and stained for rabbit polyclonal anti-HDAC1-11 (red) and goat polyclonal anti-β-actin (green) to highlight tissue structure. Relatively, strong staining was observed across Class I HDACs and weak staining was observed in class IIa HDACs. Strong non-specific staining of HDAC10 and HDAC11 was observed in the connective tissue of the stroma with very weak staining seen in the cells. Merged image: nucleus stained with DAPI (blue), HDAC1-11 (red), and β-actin (green). Images were acquired using an Olympus BX61 fluorescence microscope automated with FVII Camera. Bar = 200μm; x10 magnification.

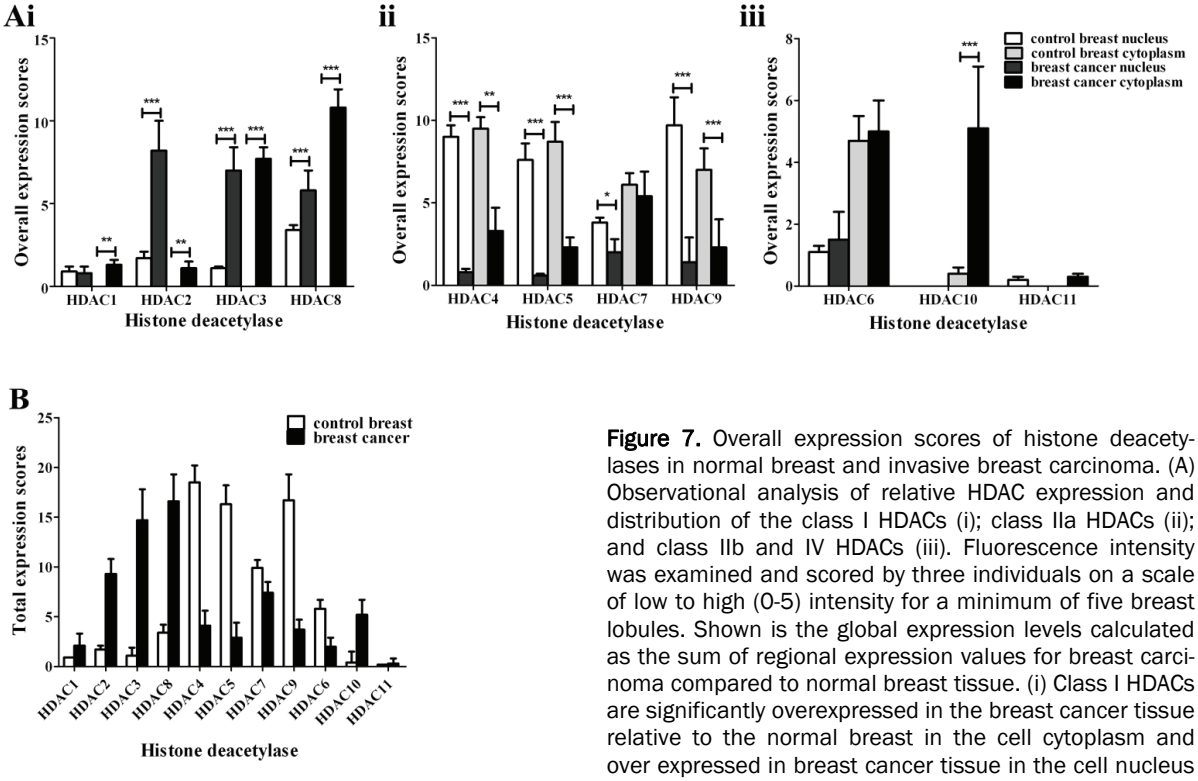

Figure 7. Overall expression scores of histone deacetylases in normal breast and invasive breast carcinoma. (A) Observational analysis of relative HDAC expression and distribution of the class I HDACs (i); class IIa HDACs (ii); and class IIb and IV HDACs (iii). Fluorescence intensity was examined and scored by three individuals on a scale of low to high (0-5) intensity for a minimum of five breast lobules. Shown is the global expression levels calculated as the sum of regional expression values for breast carcinoma compared to normal breast tissue. (i) Class I HDACs are significantly overexpressed in the breast cancer tissue relative to the normal breast in the cell cytoplasm and over expressed in breast cancer tissue in the cell nucleus for HDAC2, 3 and 8. (ii) Both HDAC5 and HADC9 are significantly decreased in the breast cancer tissue relative to the normal breast tissue in cell nucleus and cell cytoplasm. HDAC4 is significantly decreased in the cytoplasm and HDAC7 is decreased in the nucleus (iii) there are significant increases in HDAC 10 expressed in the cell cytoplasm of the cells found in the cancer breast tissue in comparison to the normal breast tissue. N=7 in control breast and n=5 in breast cancer; *P<0.05, **P<0.01, ***P<0.001. (B) Total HDAC expression scores in control breast tissue in comparison to breast cancer tissue. Class I HDAC are overexpressed in the breast cancer and class IIa HDACs are under expressed. HDAC8 is most expressed in breast cancer tissue and HDAC4 is most expressed in normal breast tissue.

pression and with ER and PR receptor expression [41, 44]. Similarly, it has been shown that HDAC6 mRNA is expressed at significantly high levels in breast cancer patients with ERα and PR positive tumours that are small (less than 2cm) and have low histological grade [33, 38].

To investigate to heterogeneity of the ductal carcinoma cells found in the breast tissue we analysed 100 individual cells for expression of each HDAC enzyme, comparing the expression levels in the overall cell and the nucleus. We found marked heterogeneity, particularly in the expression of class I HDACs (**Figures 8A** and **8B**). This could have implications for therapy given that heterogeneous expression could translate to differences in sensitivities to HDAC inhibitors.

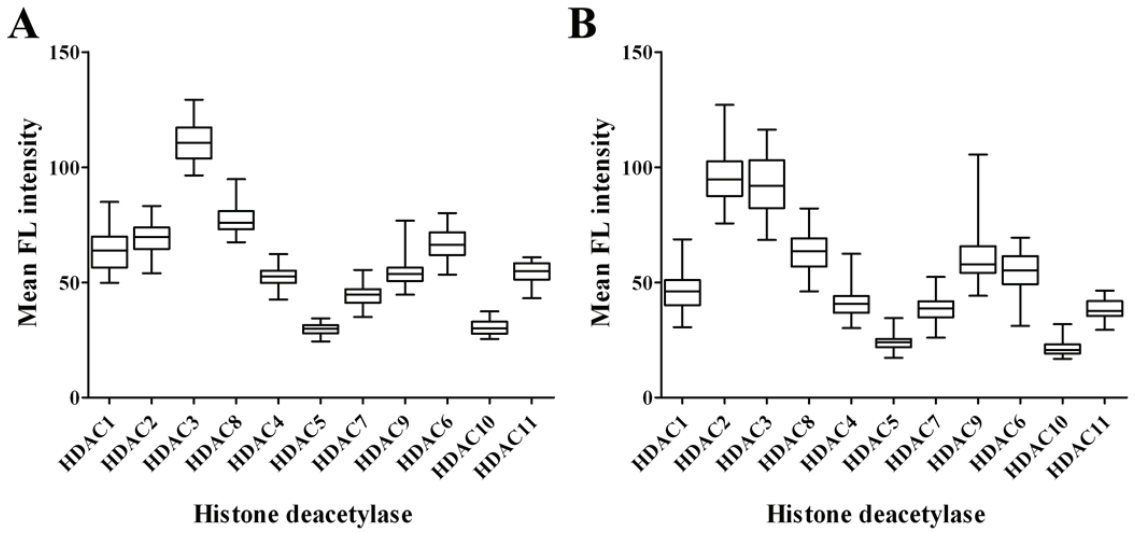

Figure 8. The relative distribution of histone deacetylase expression in ductal carcinoma cells in breast tissue. Breast carcinoma tissue stained with HDAC1-11 as described in the materials and methods. Immunofluorescence analysis was performed using Image J software to measure the mean fluorescence intensity of the expression of each HDAC the whole cell (A) or the nucleus (B) in 100 individual ductal carcinoma cells. Shown are box plots of the fluorescence intensity values for each HDAC. (A) Class I HDACs showed the greatest amount of variability in HDAC expression within cancer cells of breast tissue, with HDAC1 and HDAC3 showing the largest amount of heterogeneity. (B) In comparison greater variability of HDAC expression between cells was seen within the nucleus for the different HDACs.

To investigate HDAC expression in control and breast tissue we used an anti-HDAC1-11 family kit (Biovision). We validated our findings with different primary antibodies; rabbit anti-HDAC4 (Epitomics) and mouse anti-HDAC8 (Sigma). We found staining to be similar between the different antibodies (**Figure 9**). We also stained for EGFr and transferrin receptors as controls. We found very weak staining of EGFr isoform pT693 and s695 in control breast tissue and strong staining in the epithelial carcinoma cells in the breast tissue (**Figure 10A**). Disparate staining of the transferrin receptor (CD71) was observed in normal breast cancer tissue (**Figure 10Bi**) with stronger staining found localized in the ducts. Sporadic staining of transferrin receptors was also observed in the cancer breast tissue (**Figure 10Bii**). Finally, annexin V staining was used to detect cells that expressed phosphatidylserine on the cell surface, a hallmark of apoptosis. We found minimal staining of Annexin V in lobules and vasculature of the control breast tissue (**Figure 11A** and **11B**) and strong staining in breast regions of invasive breast carcinoma (**Figure 11C**) and medium staining in a lobule in breast cancer tissue (**Figure 11D**). This suggests that the epithelial cancer cells found in the breast cancer tissue have a higher predisposition to apoptosis in comparison to normal breast cells.

In general, our findings indicate elevated expression of class I HDACs compared to class II enzymes in breast cancer tissue. This may suggest the potential benefit of the use of class I selective inhibitors in therapy. For example, MS-275 (Entinostat), a class I specific HDAC inhibitor is currently in phase II clinical trials and has been shown to inhibit breast cancer tumour growth, angiogenesis and metastasis [46, 47]. However, analysis of individual cancer cells in the same tissue indicated marked heterogeneity in the expression of most class I enzymes indicating potential complications for therapy. Overall, much further research is required to clarify the expression and functional roles of the metal-dependent HDAC enzymes in cancer. Our immunofluorescence approach can be utilized to rapidly compare, in an unbiased semi-quantitative manner, the differential levels of expression of HDAC enzymes in cells and tissues using widely available imaging software. It is anticipated that such analysis will become increasingly important as more class- or isoform -specific histone deacetylase inhibitors become

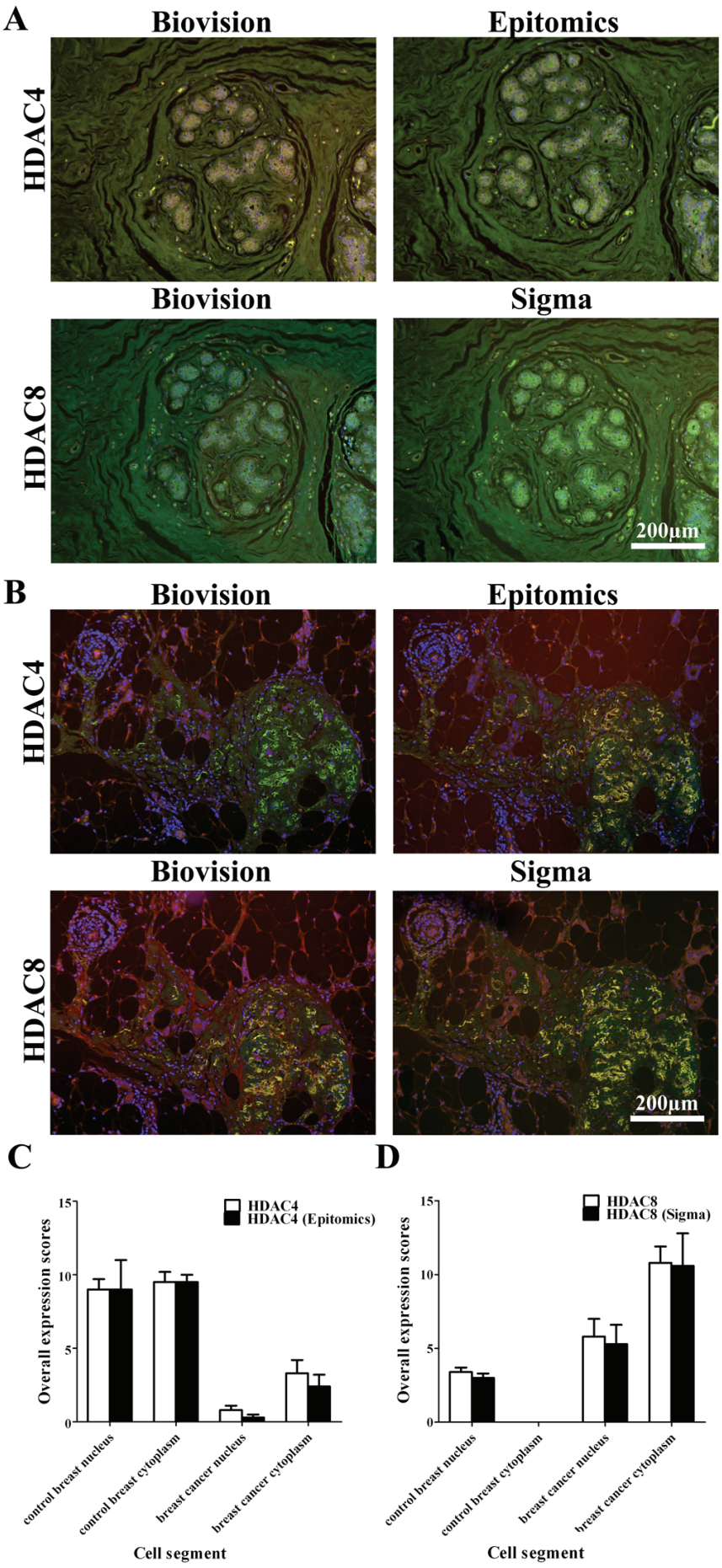

Figure 9. Comparison of HDAC4 and 8 using two different antibodies. Immunofluorescence images of control breast (A) and breast cancer (B) stained with polyclonal rabbit anti-HDAC4 (Biovision); monoclonal rabbit anti-HDAC4 (Epitomics); polyclonal rabbit anti-HDAC8 (Biovision) and monoclonal mouse anti-HDAC8 (Sigma). Merged image: nucleus stained with DAPI (blue), HDAC4, 8 (red), β-actin (green). Images were acquired using an Olympus BX61 fluorescence microscope automated with FVII Camera at x20 magnification. Bar = 200µm; x10 magnification. Overall expression levels of HDAC4 (C) and HDAC8 (D) calculated as the sum of regional expression values for invasive breast carcinoma against control breast tissue.

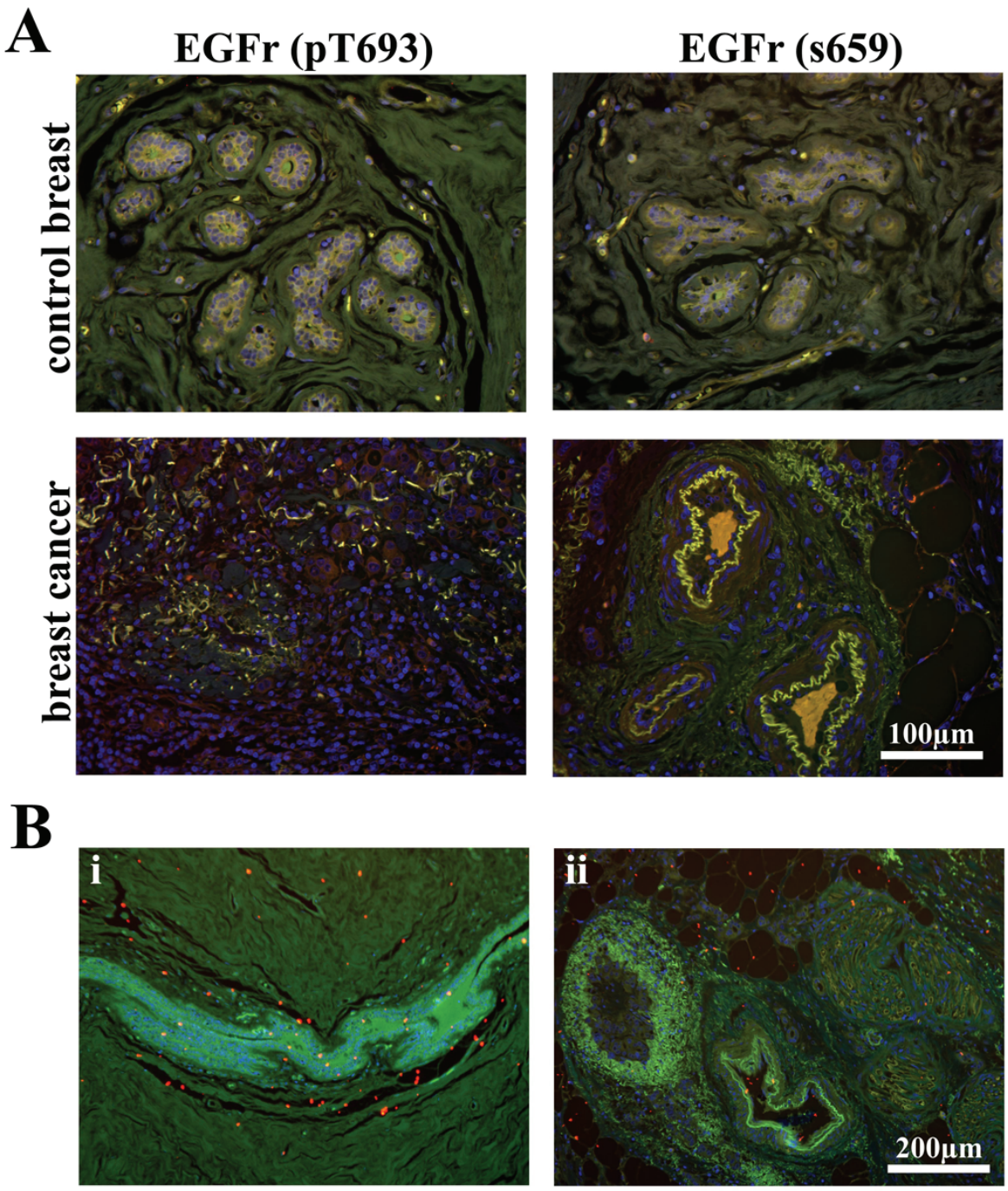

Figure 10. Distribution of epidermal growth factor and transferrin receptors in control and breast cancer tissue. Representative tissues were stained with (A) monoclonal rabbit anti-phospho-EGFr (pT693); polyclonal rabbit anti-phosho-EGFr (s695) (B) and monoclonal rabbit anti-CD71 (TFRC). (A) Weak staining of both EGFr (pT693) and EGFr (s659) was observed in the control breast tissue in contrast to strong staining observed in the invasive breast carcinoma tissue. (C) Control breast expressing transferrin receptor (red) (i) showed relatively equal amounts of expression in breast cancer (ii). Merged image: nucleus stained with DAPI (blue), EGFr and CD71 (red), β-actin (green). Images were acquired using an Olympus BX61 fluorescence microscope with automated FVII camera. Bar = 200µm, 100µm; x10, x20 magnification respectively.

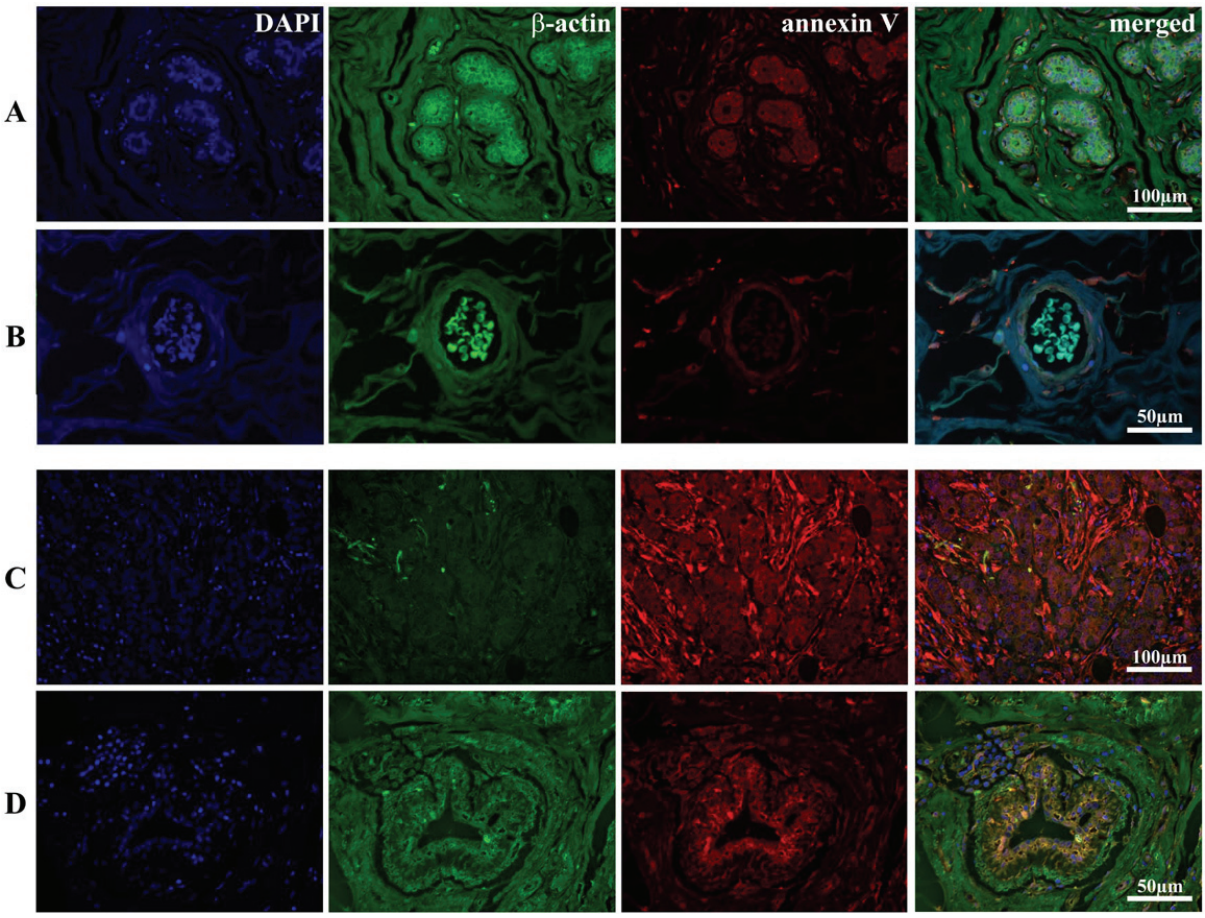

Figure 11. Invasive breast cancer has a higher predisposition to apoptosis in comparison to control breast cancer cells. Immunofluorescence staining for a membrane apoptotic marker, Annexin V (red) is shown in representative control and breast cancer tissue sections. Goat polyclonal anti-β-actin (green) was used to highlight the cytoskeleton. (A) Weak Annexin V staining was observed in the columnar epithelial cells of ductules in the control breast and (B) very weak staining was seen in epithelium of blood vessels in the stroma of the control breast. (C) In contrast, strong staining was seen in an invasive ductal carcinoma mass where high concentrations of malignant cells are found. (D) Strong staining of Annexin V in the columnar epithelial cells of a ductule in a tissue region of invasive ductal carcinoma. Merged image: nucleus stained with DAPI (blue), Annexin V (red), β-actin (green). Images were acquired using an Olympus BX61 fluorescence microscope with automated FVII camera. Bar = 200μm, 100μm; x10, x20 magnification respectively.

readily available.

Acknowledgements

The support of the Australian Institute of Nuclear Science and Engineering is acknowledged. TCK was the recipient of AINSE awards. Epigenomic Medicine Laboratory is supported by the National Health and Medical Research Council of Australia. KV is supported by a Baker IDI postgraduate scholarship. Supported in part by the Victorian Government's Operational Infrastructure Support Program. The authors would like to acknowledge the use of the facilities provided by Monash Micro Imaging @ AMREP and particularly, the expert assistance from Drs Stephen Cody and Iśka Carmichael. Both KV and TCK declare that they have no direct financial relation with the commercial identities mentioned in this manuscript that might lead to a conflict of interest.

Address correspondence to: Dr. Tom Karagiannis, Epigenomic Medicine, BakerIDI Heart and Diabetes Institute, 75 Commercial Road, Melbourne, VIC, Aus-

tralia Tel: +613 8532 1309; Fax: +613 8532 1100; E-mail: tom.karagiannis@bakeridi.edu.au

References

[1] Kuo MH, Allis CD. Roles of histone acetyltransferases and deacetylases in gene regulation. Bioessays 1998; 20: 615-626.

[2] Cyr AR, Domann FE. The redox basis of epigenetic modifications: from mechanisms to functional consequences. Antioxid Redox Signal 2011; 15: 551-589.

[3] Wade PA, Pruss D and Wolffe AP. Histone acetylation: chromatin in action. Trends Biochem Sci 1997; 22: 128-132.

[4] Glozak MA, Sengupta N, Zhang X and Seto E. Acetylation and deacetylation of non-histone proteins. Gene 2005; 363: 15-23.

[5] Cheung P, Allis CD and Sassone-Corsi P. Signaling to chromatin through histone modifications. Cell 2000; 103: 263-271.

[6] Hildmann C, Riester D and Schwienhorst A. Histone deacetylases-an important class of cellular regulators with a variety of functions. Appl Microbiol Biotechnol 2007; 75: 487-497.

[7] Clayton AL, Hazzalin CA and Mahadevan LC. Enhanced histone acetylation and transcription: a dynamic perspective. Mol Cell 2006; 23: 289-296.

[8] Allis CD, Berger SL, Cote J, Dent S, Jenuwien T, Kouzarides T, Pillus L, Reinberg D, Shi Y, Shiekhattar R, Shilatifard A, Workman J and Zhang Y. New nomenclature for chromatin-modifying enzymes. Cell 2007; 131: 633-636.

[9] Dokmanovic M, Marks PA. Prospects: histone deacetylase inhibitors. J Cell Biochem 2005; 96: 293-304.

[10] Rosato RR, Grant S. Histone deacetylase inhibitors: insights into mechanisms of lethality. Expert Opin Ther Targets 2005; 9: 809-824.

[11] Minucci S, Pelicci PG. Histone deacetylase inhibitors and the promise of epigenetic (and more) treatments for cancer. Nat Rev Cancer 2006; 6: 38-51.

[12] Xu WS, Parmigiani RB and Marks PA. Histone deacetylase inhibitors: molecular mechanisms of action. Oncogene 2007; 26: 5541-5552.

[13] Landry J, Sutton A, Tafrov ST, Heller RC, Stebbins J, Pillus L and Sternglanz R. The silencing protein SIR2 and its homologs are NAD-dependent protein deacetylases. Proc Natl Acad Sci USA 2000; 97: 5807-5811.

[14] Haigis MC, Guarente LP. Mammalian sirtuins-emerging roles in physiology, aging, and calorie restriction. Genes Dev 2006; 20: 2913-2921.

[15] Landry J, Slama JT and Sternglanz R. Role of NAD(+) in the deacetylase activity of the SIR2-like proteins. Biochem Biophys Res Commun 2000; 278: 685-690.

[16] Gregoretti IV, Lee YM and Goodson HV. Molecular evolution of the histone deacetylase family: functional implications of phylogenetic analysis. J Mol Biol 2004; 338: 17-31.

[17] Bolden JE, Peart MJ and Johnstone RW. Anticancer activities of histone deacetylase inhibitors. Nat Rev Drug Discov 2006; 5: 769-784.

[18] Marks P, Rifkind RA, Richon VM, Breslow R, Miller T and Kelly WK. Histone deacetylases and cancer: causes and therapies. Nat Rev Cancer 2001; 1: 194-202.

[19] Yang XJ, Seto E. Collaborative spirit of histone deacetylases in regulating chromatin structure and gene expression. Curr Opin Genet Dev 2003; 13: 143-153.

[20] Martin M, Kettmann R and Dequiedt F. Class IIa histone deacetylases: regulating the regulators. Oncogene 2007; 26: 5450-5467.

[21] Witt O, Deubzer HE, Milde T and Oehme I. HDAC family: What are the cancer relevant targets? Cancer Lett 2009; 277: 8-21.

[22] Dokmanovic M, Clarke C and Marks PA. Histone deacetylase inhibitors: overview and perspectives. Mol Cancer Res 2007; 5: 981-989.

[23] Mai A, Rotili D, Valente S and Kazantsev AG. Histone deacetylase inhibitors and neurodegenerative disorders: holding the promise. Curr Pharm Des 2009; 15: 3940-3957.

[24] Marks PA. Histone deacetylase inhibitors: a chemical genetics approach to understanding cellular functions. Biochim Biophys Acta 2010; 1799: 717-725.

[25] Marks PA, Xu WS. Histone deacetylase inhibitors: Potential in cancer therapy. J Cell Biochem 2009; 107: 600-608.

[26] de Ruijter AJ, van Gennip AH, Caron HN, Kemp S and van Kuilenburg AB. Histone deacetylases (HDACs): characterization of the classical HDAC family. Biochem J 2003; 370: 737-749.

[27] Gao YS, Hubbert CC and Yao TP. The microtubule-associated histone deacetylase 6 (HDAC6) regulates epidermal growth factor receptor (EGFR) endocytic trafficking and degradation. J Biol Chem 2010; 285: 11219-11226.

[28] Hubbert C, Guardiola A, Shao R, Kawaguchi Y, Ito A, Nixon A, Yoshida M, Wang XF and Yao TP. HDAC6 is a microtubule-associated deacetylase. Nature 2002; 417: 455-458.

[29] Kawaguchi Y, Kovacs JJ, McLaurin A, Vance JM, Ito A and Yao TP. The deacetylase HDAC6 regulates aggresome formation and cell viability in response to misfolded protein stress. Cell 2003; 115: 727-738.

[30] Marks PA, Breslow R. Dimethyl sulfoxide to vorinostat: development of this histone deacetylase inhibitor as an anticancer drug. Nat Biotechnol 2007; 25: 84-90.

[31] Campas-Moya C. Romidepsin for the treatment of cutaneous T-cell lymphoma. Drugs Today (Barc) 2009; 45: 787-795.

[32] Nakagawa M, Oda Y, Eguchi T, Aishima S, Yao T, Hosoi F, Basaki Y, Ono M, Kuwano M, Tanaka M and Tsuneyoshi M. Expression profile of

class I histone deacetylases in human cancer tissues. Oncol Rep 2007; 18: 769-774.
[33] Azuma K, Urano T, Horie-Inoue K, Hayashi S, Sakai R, Ouchi Y and Inoue S. Association of estrogen receptor alpha and histone deacetylase 6 causes rapid deacetylation of tubulin in breast cancer cells. Cancer Res 2009; 69: 2935-2940.
[34] Meng Q, Chen X, Sun L, Zhao C, Sui G and Cai L. Carbamazepine promotes Her-2 protein degradation in breast cancer cells by modulating HDAC6 activity and acetylation of Hsp90. Mol Cell Biochem 2011; 348: 165-171.
[35] Rey M, Irondelle M, Waharte F, Lizarraga F and Chavrier P. HDAC6 is required for invadopodia activity and invasion by breast tumor cells. Eur J Cell Biol 2011; 90: 128-135.
[36] Saji S, Kawakami M, Hayashi S, Yoshida N, Hirose M, Horiguchi S, Itoh A, Funata N, Schreiber SL, Yoshida M and Toi M. Significance of HDAC6 regulation via estrogen signaling for cell motility and prognosis in estrogen receptor-positive breast cancer. Oncogene 2005; 24: 4531-4539.
[37] Wang KH, Kao AP, Chang CC, Lee JN, Hou MF, Long CY, Chen HS and Tsai EM. Increasing CD44+/CD24(-) tumor stem cells, and upregulation of COX-2 and HDAC6, as major functions of HER2 in breast tumorigenesis. Mol Cancer 2010; 9: 288.
[38] Zhang Z, Yamashita H, Toyama T, Sugiura H, Omoto Y, Ando Y, Mita K, Hamaguchi M, Hayashi S and Iwase H. HDAC6 expression is correlated with better survival in breast cancer. Clin Cancer Res 2004; 10: 6962-6968.
[39] Park SY, Jun JA, Jeong KJ, Heo HJ, Sohn JS, Lee HY, Park CG and Kang J. Histone deacetylases 1, 6 and 8 are critical for invasion in breast cancer. Oncol Rep 2011; 25: 1677-1681.
[40] Hsieh TH, Tsai CF, Hsu CY, Kuo PL, Lee JN, Chai CY, Wang SC and Tsai EM. Phthalates induce proliferation and invasiveness of estrogen receptor-negative breast cancer through the AhR/HDAC6/c-Myc signaling pathway. FASEB J 2011.
[41] Krusche CA, Wulfing P, Kersting C, Vloet A, Bocker W, Kiesel L, Beier HM and Alfer J. Histone deacetylase-1 and -3 protein expression in human breast cancer: a tissue microarray analysis. Breast Cancer Res Treat 2005; 90: 15-23.
[42] Normanno N, De Luca A, Bianco C, Strizzi L, Mancino M, Maiello MR, Carotenuto A, De Feo G, Caponigro F and Salomon DS. Epidermal growth factor receptor (EGFR) signaling in cancer. Gene 2006; 366: 2-16.
[43] Crow MJ, Grant G, Provenzale JM and Wax A. Molecular imaging and quantitative measurement of epidermal growth factor receptor expression in live cancer cells using immunolabeled gold nanoparticles. AJR Am J Roentgenol 2009; 192: 1021-1028.
[44] Weichert W. HDAC expression and clinical prognosis in human malignancies. Cancer Lett 2009; 280: 168-176.
[45] Feng W, Lu Z, Luo RZ, Zhang X, Seto E, Liao WS and Yu Y. Multiple histone deacetylases repress tumor suppressor gene ARHI in breast cancer. Int J Cancer 2007; 120: 1664-1668.
[46] Cai FF, Kohler C, Zhang B, Wang MH, Chen WJ and Zhong XY. Epigenetic therapy for breast cancer. Int J Mol Sci 2011; 12: 4465-4487.
[47] Camphausen K, Burgan W, Cerra M, Oswald KA, Trepel JB, Lee MJ and Tofilon PJ. Enhanced radiation-induced cell killing and prolongation of gammaH2AX foci expression by the histone deacetylase inhibitor MS-275. Cancer Res 2004; 64: 316-321.